ONLINE DATA SUPPLEMENT

Doxorubicin blocks cardiomyocyte autophagic flux by inhibiting lysosome acidification

Dan L. Li[1], Zhao V. Wang[1], Guanqiao Ding[1], Wei Tan[2], Xiang Luo[1], Alfredo Criollo[1], Min Xie[1], Nan Jiang[1], Herman May[1], Viktoriia Kyrychenko[1], Jay W. Schneider[1], Thomas G. Gillette[1], Joseph A. Hill[1,2]

Correspondence:
Joseph A. Hill, MD, PhD
Division of Cardiology
UT Southwestern Medical Center
NB11.200
6000 Harry Hines Blvd
Dallas, TX 75390-8573
Tel: 214.648.1400
Fax: 214.648.1450
joseph.hill@utsouthwestern.edu

Supplemental Figure 1. A mouse model of chronic doxorubicin cardiomyopathy without systemic toxicity.

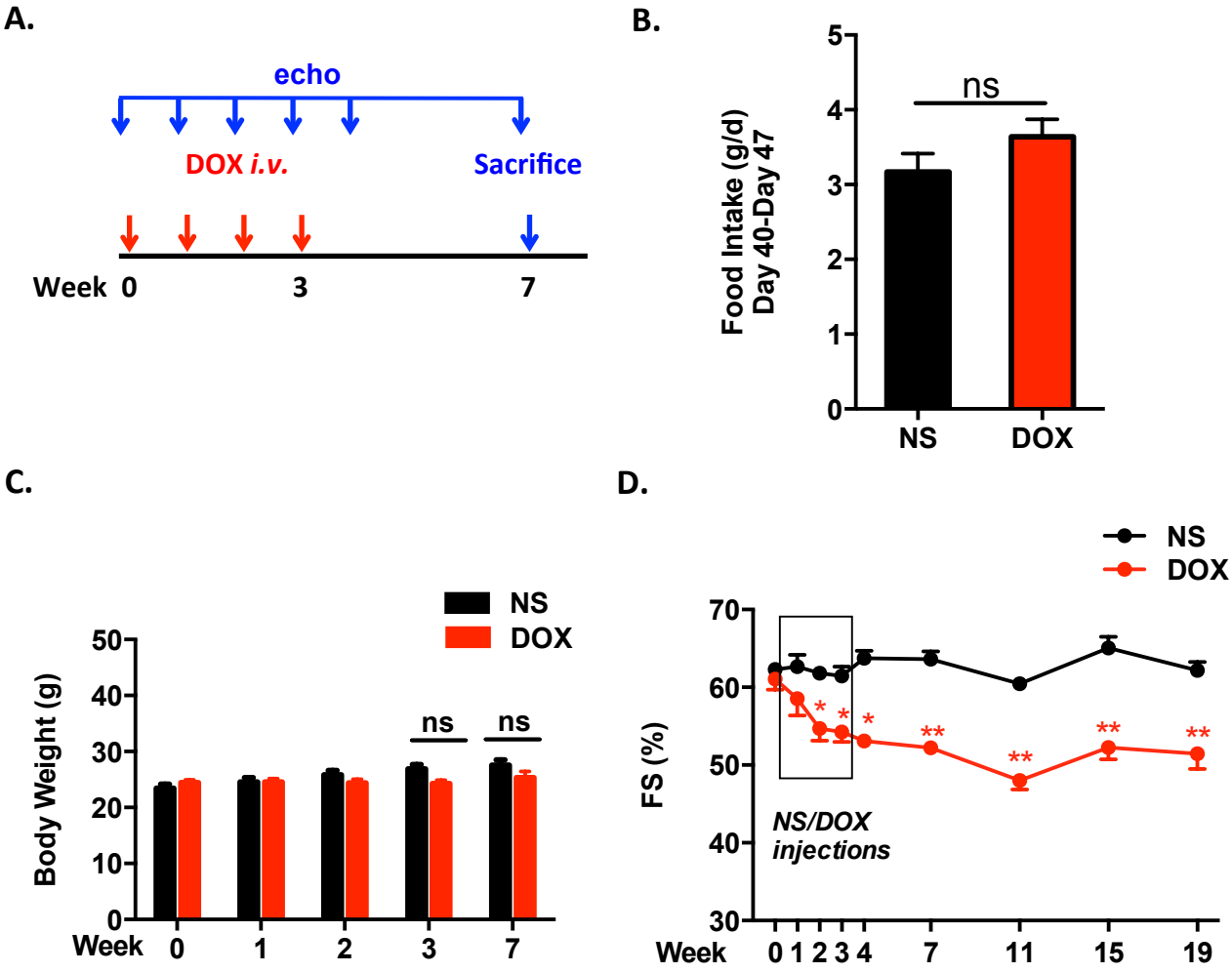

Supplemental Figure 2. Doxorubicin inhibits autophagic flux in mouse heart

A.

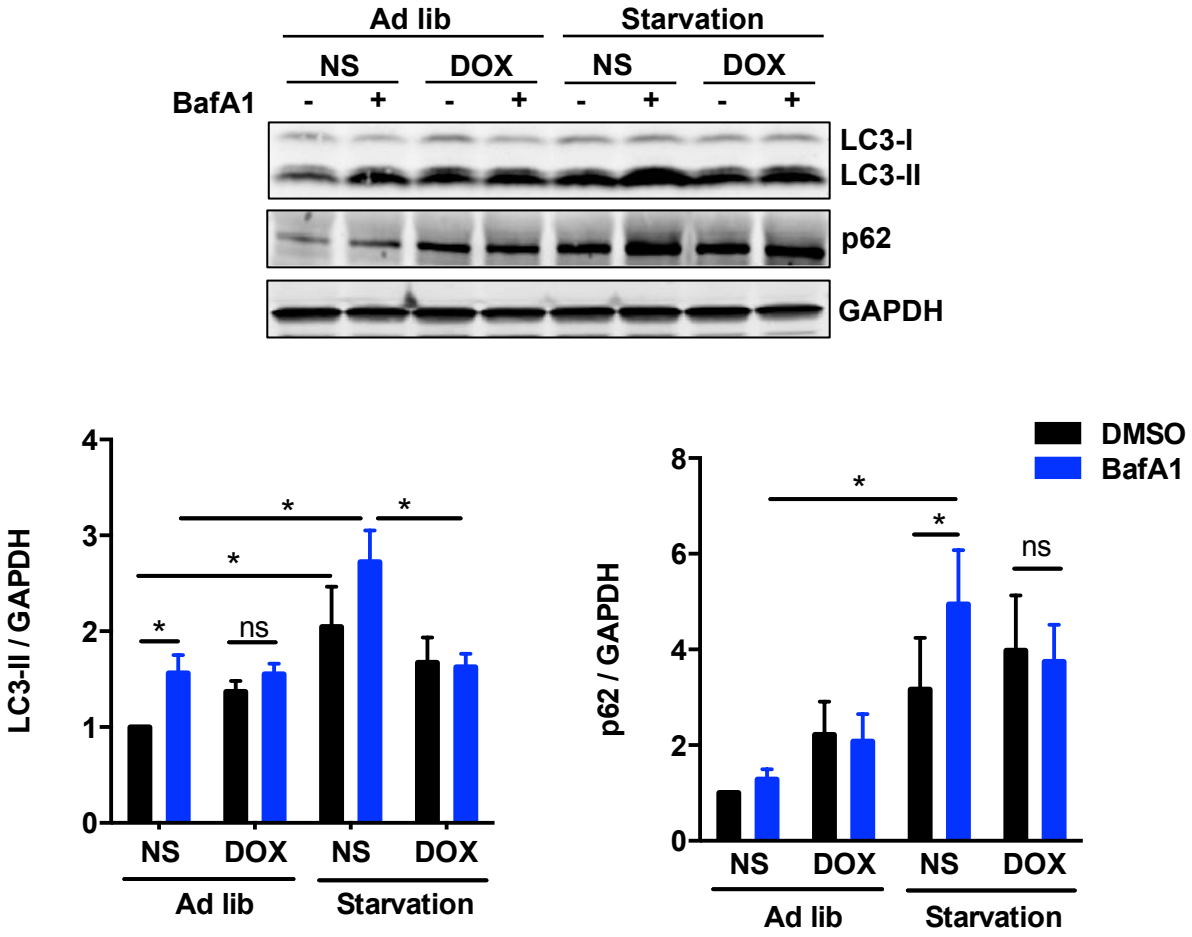

B.

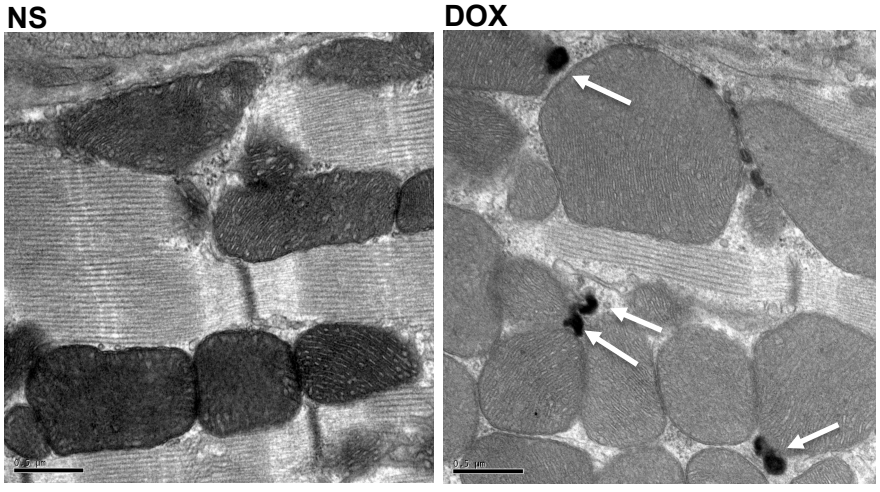

Supplemental Figure 3. Doxorubicin inhibits autophagic flux in cultured cardiomyocytes.

A.

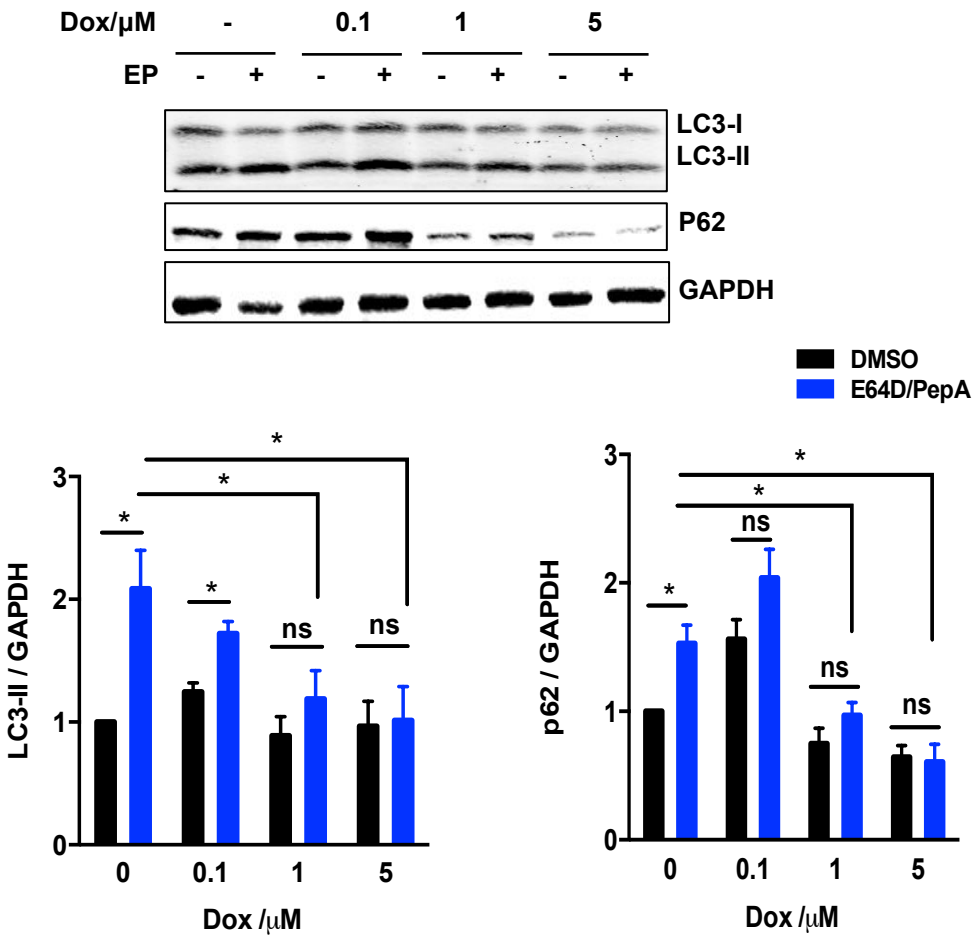

B.

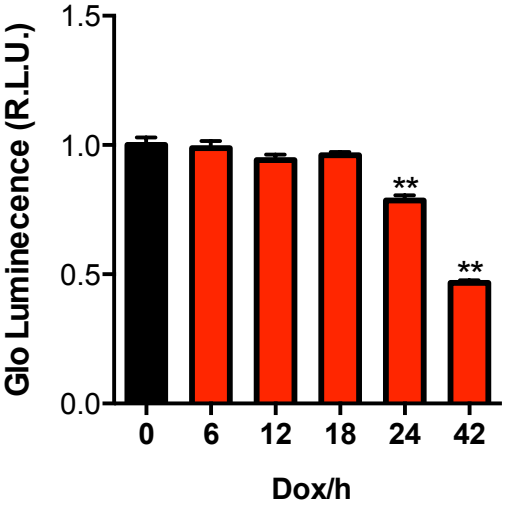

Supplemental Figure 3. Continued.

C.

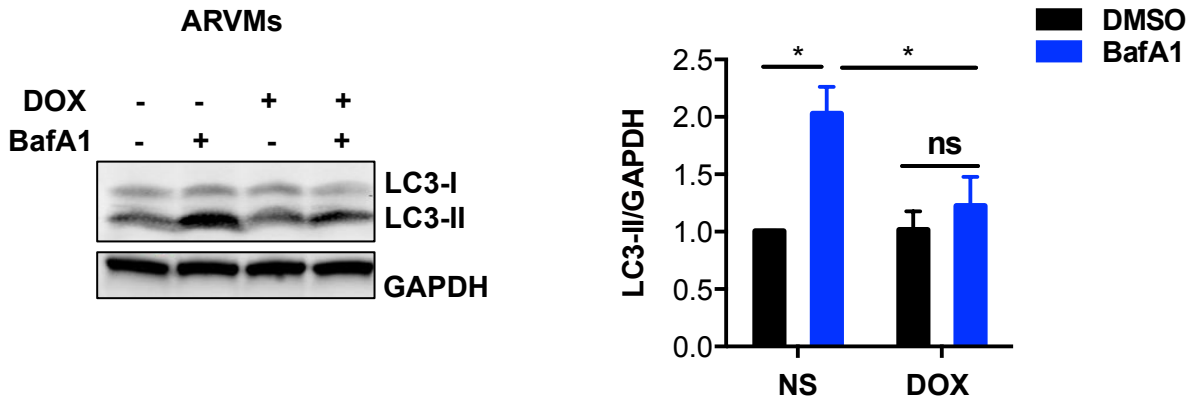

D.

Cardiomyocyte-like cells differentiated from H9 human embryonic stem cells

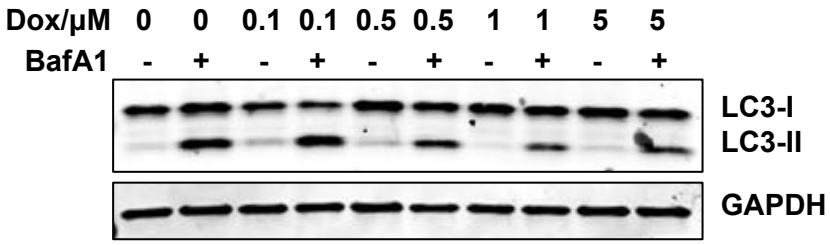

E.

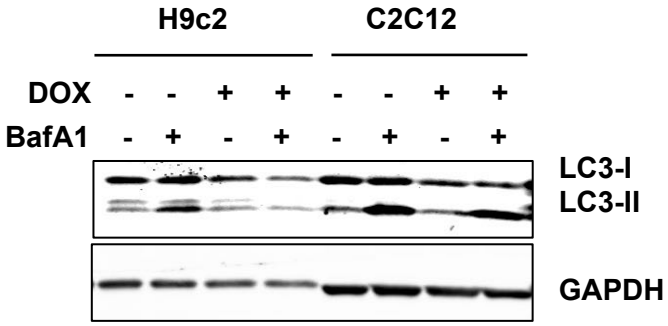

Supplemental figure 4. mTORC1 activation is not required for inhibition of cardiomyocyte autophagic flux by doxorubicin.

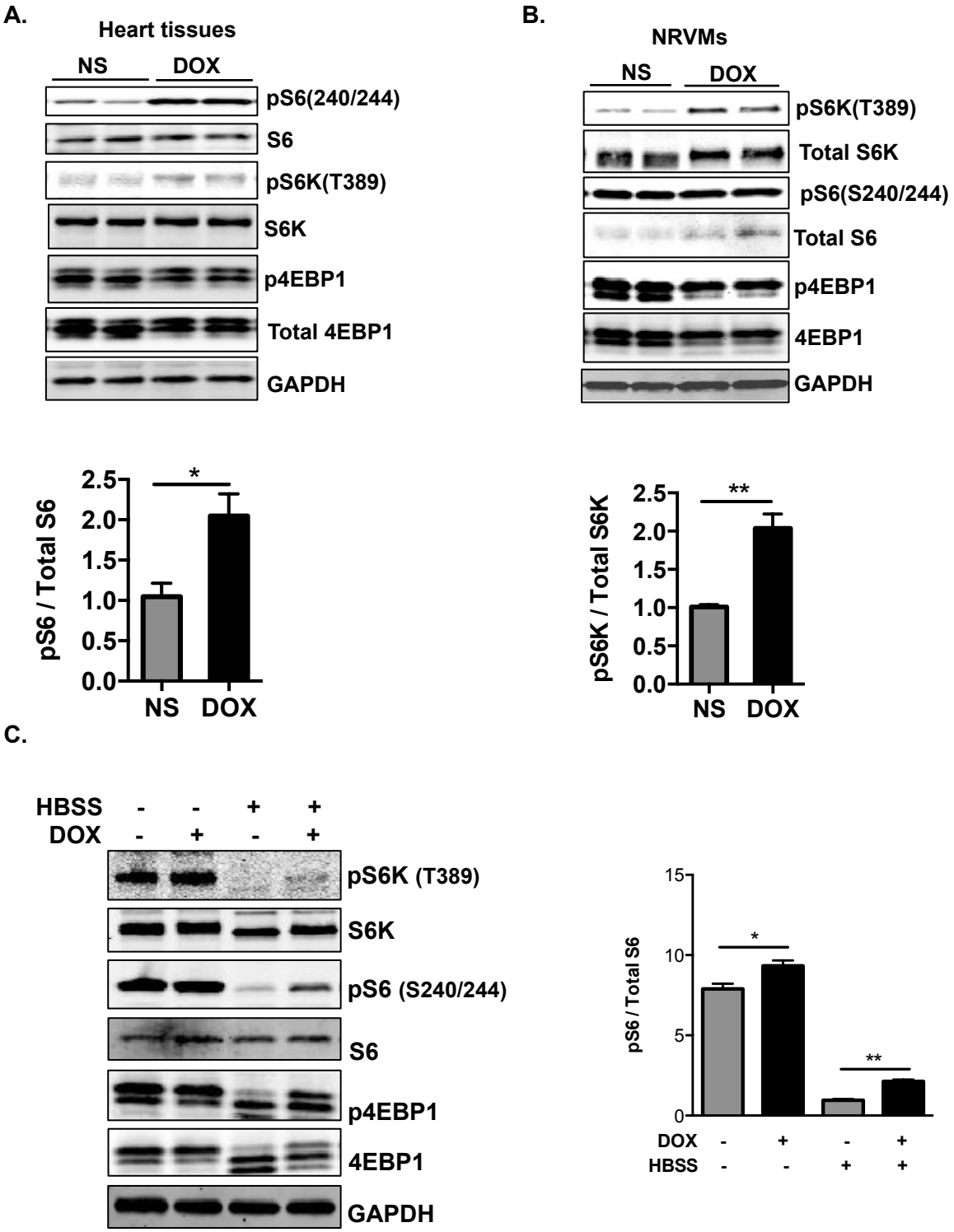

Supplemental figure 4. Continued.

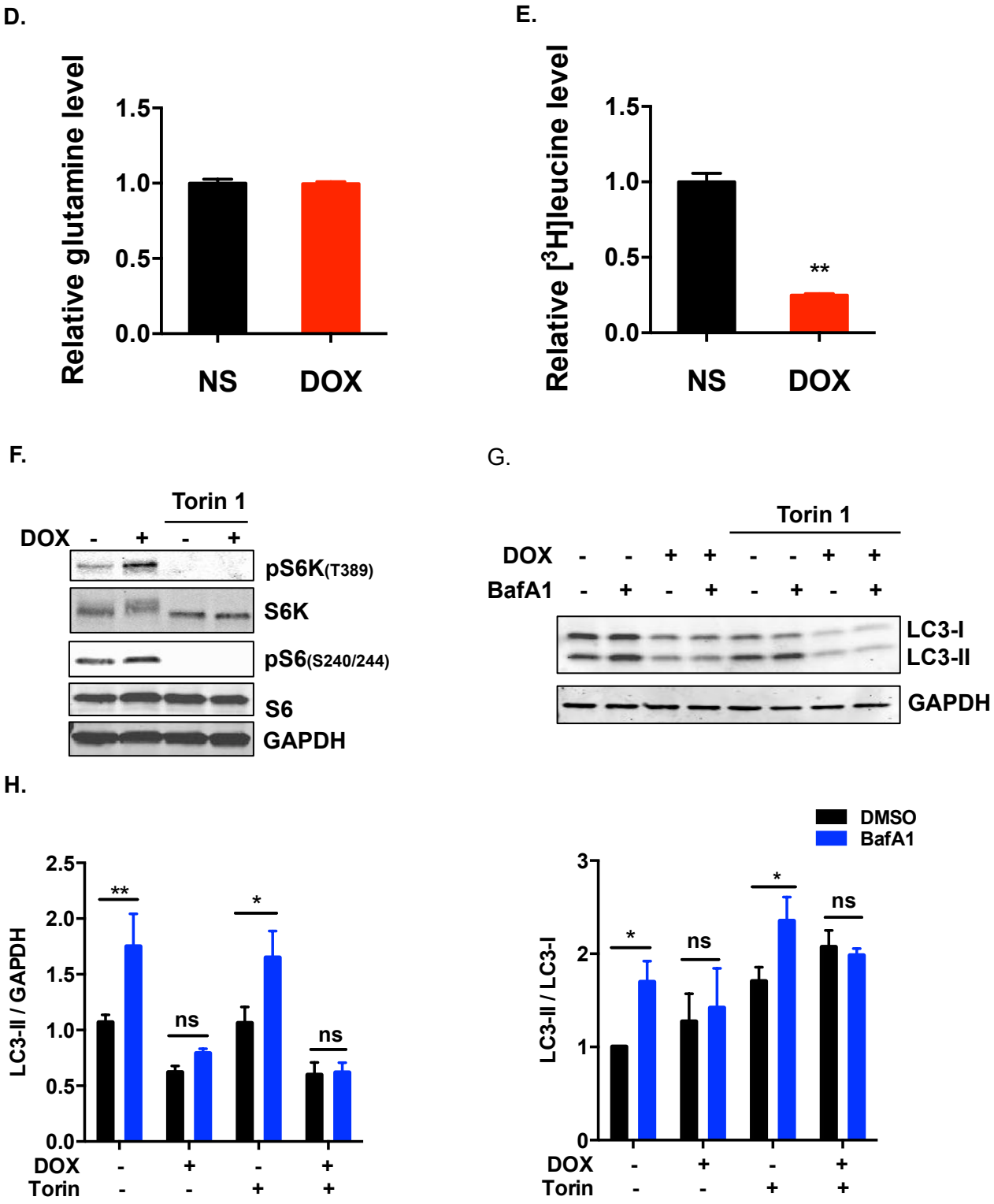

Supplemental figure 5. Doxorubicin inhibits lysosomal acidification in NRVMs.

A.

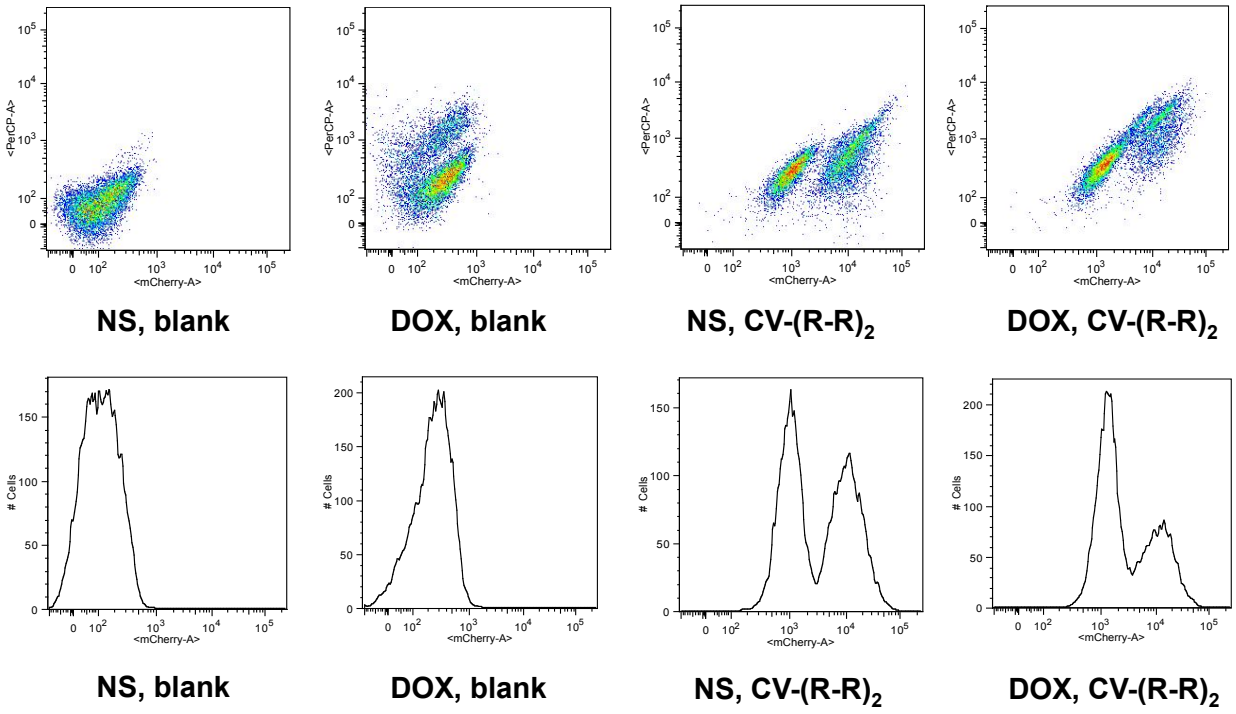

B.

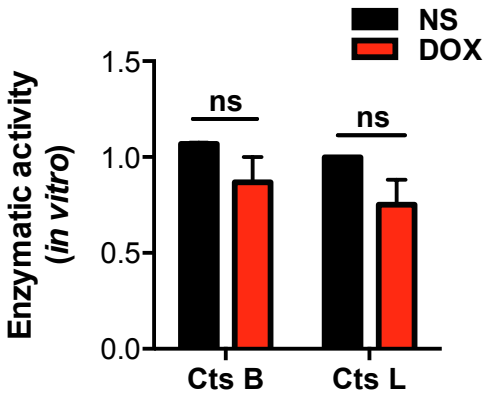

C.

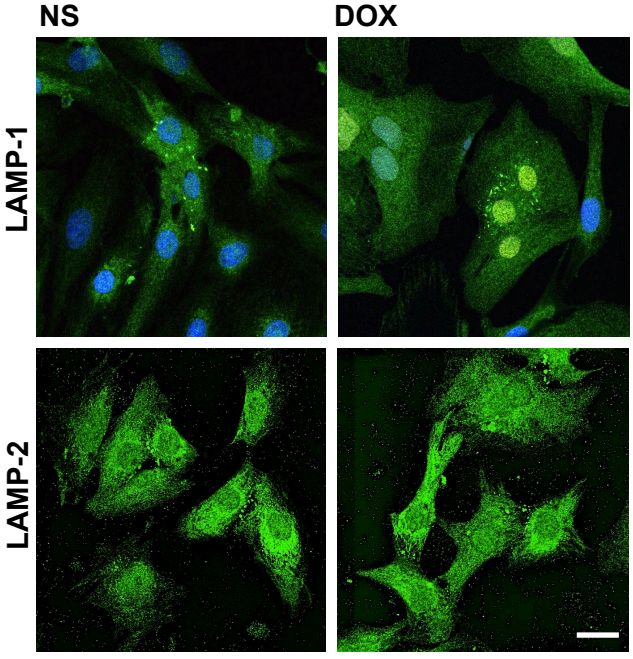

Supplemental figure 5. Continued.

D.

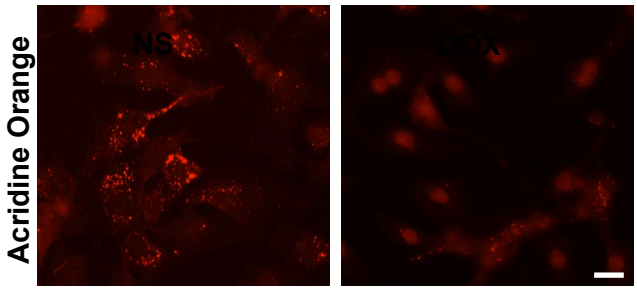

E.

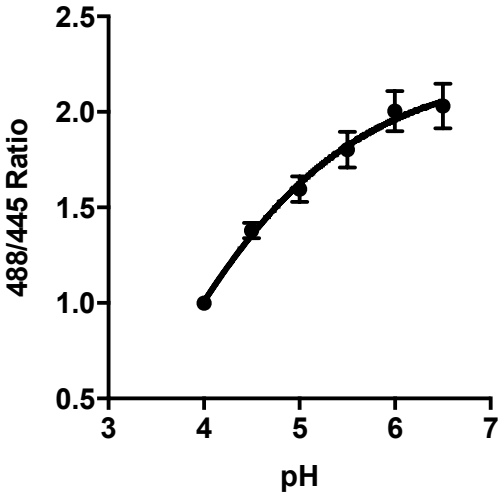

F.

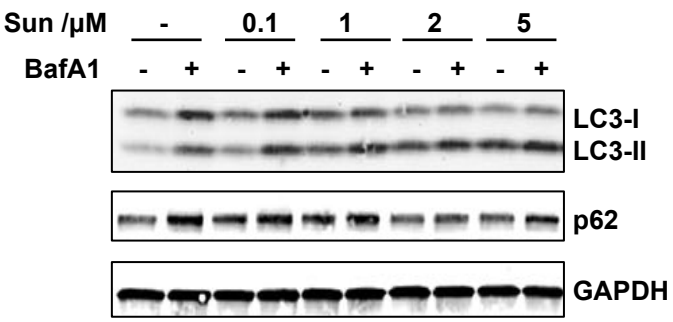

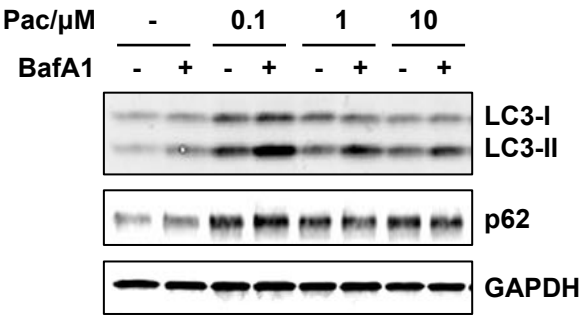

G.

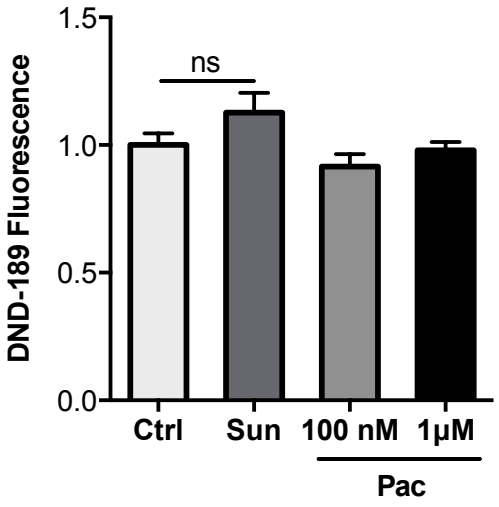

H.

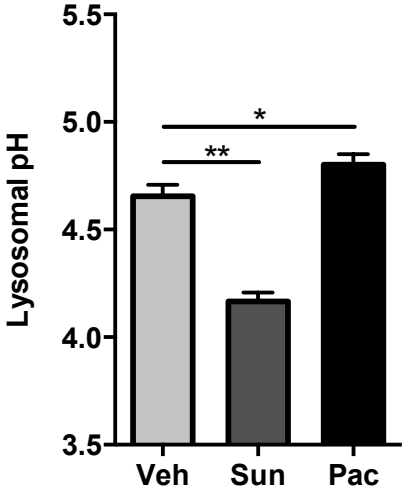

Supplemental figure 6. Beclin 1 or Atg 7 knock down in NRVMs does not correct lysosomal acidification impaired by doxorubicin.

A.

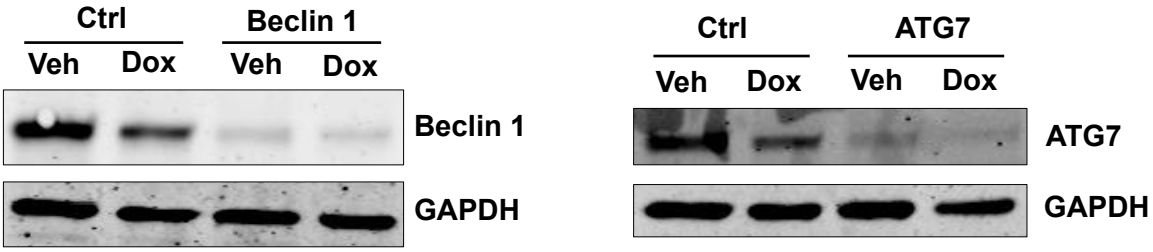

B.

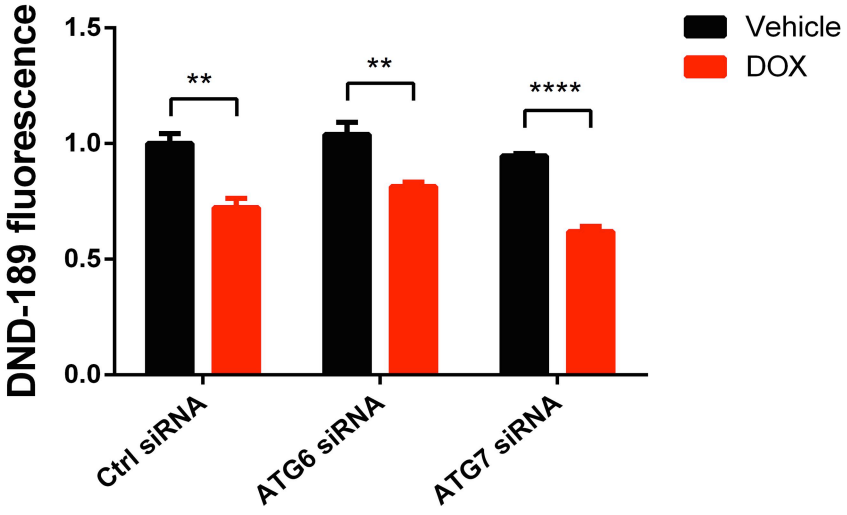

Supplemental Figure 7. Cardiomyocyte Beclin1 expression levels affect doxorubicin-induced cardiac fibrosis.

A.

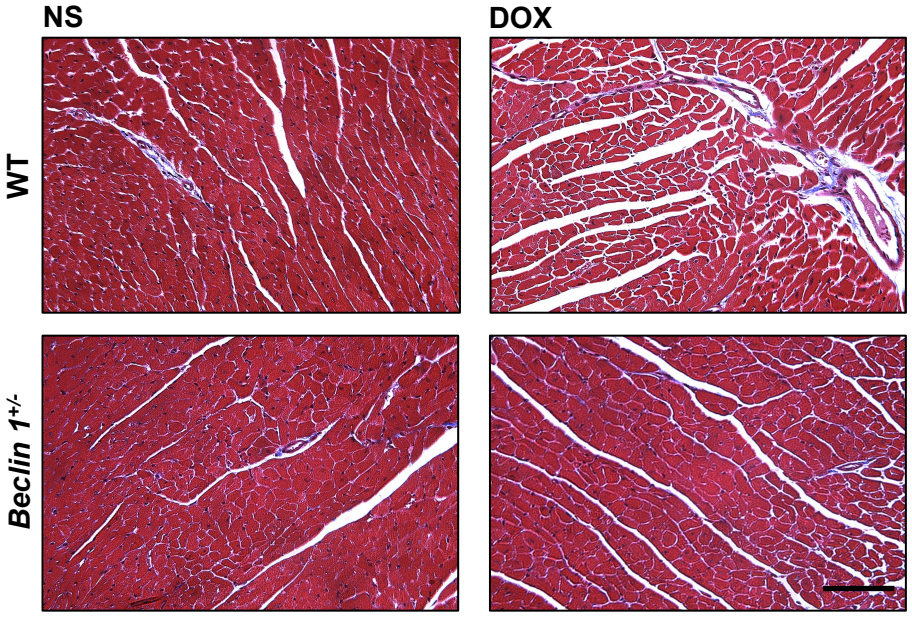

B.

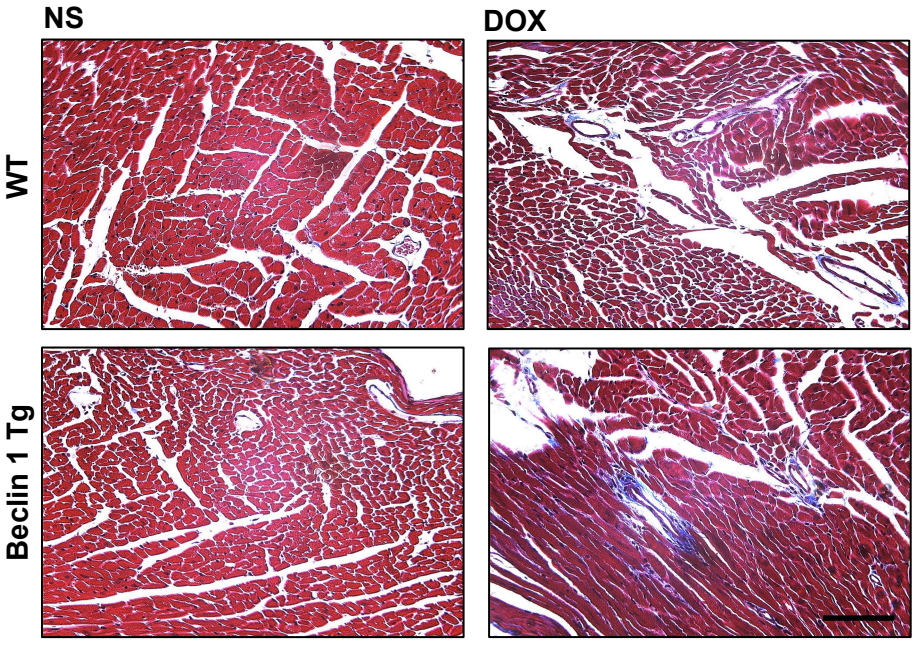

Supplemental Figure 1. **A mouse model of chronic doxorubicin cardiomyopathy without systemic toxicity.** (**A**) Schematic of chronic doxorubicin administration protocol. C57BL/6 mice of 8 to 9-weeks of age were subjected to four serial doxorubicin (5 mg/kg) injections weekly via tail vein. Echocardiography was used to examine cardiac functions before each injection, as well as at 1 and 4 weeks after the 4^{th} dose (on day 0, 6, 13, 20, and 48). Mice were sacrificed on day 49, 7 weeks after the initial injection (4 weeks after the last injection). (**B**) Food intake after treatment was not reduced in doxorubicin group. An average of food intake from day 41 to day 47 was calculated for each mouse. N = 8 mice per group. (**C**) Doxorubicin did not affect body weight following this protocol. N = 10-13 in each group. (**D**) Long term follow up of cardiac function revealed that doxorubicin-treated mice developed chronic cardiomyopathy. N = 10 per group. FS, Fractional Shortening. Repeated measures ANOVA was performed between NS and DOX groups for different time points. *, $p < 0.05$ versus control; ns, not significant.

Supplemental Figure 2. **Alteration of cardiomyocyte autophagic flux by doxorubicin *in vivo*.** (**A**) Doxorubicin inhibited cardiac autophagic flux upon starvation. Mice were treated with NS or DOX, then subjected to 24-hour starvation. Bafilomycin A1 (1.5 mg/kg, BafA1) was injected IP 2 hours before sacrifice. Immunoblotting of LC3 and p62 protein is shown. N = 4 per group. Two-way ANOVA analysis followed by Tukey *post hoc* test was used to compare multiple groups. *, $p < 0.05$; **, $p < 0.01$. (**B**) Representative transmission electron microscopy images of hearts from mice 24 hours after DOX (5 mg/kg) or NS treatment. Doxorubicin-treated heart showed increased numbers of cytoplasmic vacuoles with electron-dense contents (white arrows). Scale bar, 0.5 μm. DOX, doxorubicin. NS, normal saline. BafA1, Bafilomycin A1.

Supplemental Figure 3. **Doxorubicin inhibits autophagic flux in cultured cardiomyocytes**. (**A**) Dose-dependent inhibition of autophagic flux by doxorubicin (24 hours) in NRVM, examined by immunoblotting of LC3 and p62. N = 3 independent experiments. E64d (10 μg/mL) and pepstatin A (10 μg/mL) were added for 2 hours to block lysosomal degradation. Two-way ANOVA analysis followed by Tukey *post hoc* test was used to compare multiple groups. (**B**) Doxorubicin (1 μM) does not alter ATP levels in NRVM within 24 hours of treatment. N = 3 independent experiments in triplicates. T-test was performed between NS control group and each group with different time course of doxorubicin exposure. (**C**) Doxorubicin (1 μM, 24

hours) inhibited autophagic flux in adult rat ventricular myocytes (ARVMs) examined by immunoblotting of LC3. Quantification was analyzed from 3 independent experiments. Two-way ANOVA analysis followed by Tukey *post hoc* test was used to compare multiple groups. (**D**) Overnight treatment with doxorubicin at different concentrations inhibited autophagic flux in cardiomyocyte-like cells differentiated from H9 human embryonic stem cells. (**E**) Doxorubicin (1 μM, 24 hours) inhibited autophagic flux in H9c2 cells but not in C2C12 cells (myoblasts) as determined by immunoblotting of LC3. E/P, E64d/pepstatin A. *, $p < 0.05$; **, $p < 0.01$; ns, not significant.

Supplemental Figure 4. **mTORC1 activation is not required for inhibition of cardiomyocyte autophagic flux by doxorubicin.** (**A**) The mTORC1 signaling pathway in hearts was activated 24 hours after doxorubicin injection. pS6/total S6 was quantified. N = 4 per group. T-test was performed for statistical analysis. (**B**) The mTORC1 signaling pathway in NRVM was activated by overnight doxorubicin treatment. pS6K/total S6K was quantified. N = 4 independent experiments. T-test was used for analysis. (**C**) Doxorubicin (8-hour treatment) increased mTORC1 activity even upon starvation (HBSS, 2 hours) in NRVM. N = 3 independent experiments. One-way ANOVA analysis followed by Tukey *post hoc* test was used to compare multiple groups. (**C**) Torin 1 (50 nM) inhibited basal and doxorubicin-induced mTORC1 activity. (**D**) Doxorubicin did not affect intracellular free glutamine levels; T-test was used for statistical analysis. (**E**) Doxorubicin decreased intracellular free leucine levels. T-test was used for statistical analysis. (**F**) Torin 1 effectively blocked mTORC1 activation induced by doxorubicin. (**G**) Co-treatment with Torin 1 failed to rescue doxorubicin-induced inhibition of autophagic flux in cardiomyocytes. (**H**) Quantification of LC3-II /GAPDH and LC3-II /LC3-I in (H). N = 3 independent experiments. Two-way ANOVA analysis followed by Tukey *post hoc* test was used to compare multiple groups. *, $p < 0.05$; **, $p < 0.01$; ns, not significant.

Supplemental Figure 5. Doxorubicin inhibits lysosomal acidification in NRVM. (**A**) Flow cytometry separating fluorescence signals of doxorubicin and of Cresyl violet (CV). An example is shown using CV-$(R\text{-}R)_2$ to assess cathepsin B activity in live NRVM. CV fluorescence was collected with Ex/Em 561/610 nm while fluorescence signal from doxorubicin was minimally detected in this channel. Signal in Ex/Em 561/610 nm was quantified as measurement of cathepsin B activity respectively. The same approach was used to measure cathepsin L activity with CV-$(F\text{-}R)_2$. (**B**) *In vitro* enzyme activities of cathepsin B and cathepsin L isolated from lysosomes of cardiomyocytes treated with normal saline or doxorubicin. N = 3

independent experiments. T-test was performed for statistical analysis. ns, not significant. (**C**) Representative immunofluorescence images of NRVM with LAMP-1 and LAMP-2 immunostaining after 8-hour treatment of DOX or NS. Scale bar, 10 μm. (**D**) Representative immunofluorescence images of NRVM with Acridine Orange (1 μM for 15 minutes) staining after 8-hour-treatment of DOX. Scale bar, 10 μm. (**E**) Standard curve for measuring lysosomal pH using pH sensitive dextran (Dextran, Oregon Green 514) and ratiometric imaging. An average of 10-20 cells was analyzed at each pH in each independent experiment. Scale bar, 10 μm. (**F**) Changes in cardiomyocyte autophagic flux upon treatment with cardiotoxic chemotherapeutic drugs sunitinib and paclitaxel. Immunoblotting of LC3 after overnight incubation with different concentrations of sunitinib and paclitaxel are shown. (**G**) DND-189 fluorescence by FACS after overnight treatment with sunitinib (1 μM) or paclitaxel (100 nM and 1 μM). N = 3 independent experiments. (**H**) Lysosome pH measurement by Dextran, Oregon Green 514 in cardiomyocytes after treatment with sunitinib (1 μM) or paclitaxel (1 μM). N = 100 cells in 3 independent experiments. Sun, sunitinib. Pac, paclitaxel. T-test was performed for statistical analysis between Vehicle control group and different treatment groups, respectively. *, $p < 0.05$; **, $p < 0.01$; ns, not significant.

Supplemental Figure 6. Knockdown of Beclin 1 or Atg 7 in NRVM fails to correct the lysosomal acidification impairment elicited by doxorubicin. (**A**) siRNA for Beclin 1 and Atg 7 efficiently knocked down both genes in NRVM. **(B)** Knocking down of Beclin 1 or Atg 7 did not rescue lysosomal acidification impaired by doxorubicin. Experiments were repeated 4 times with duplicate samples. One-way ANOVA analysis was applied for statistical analysis, followed by Tukey *post hoc* test was used to compare multiple groups. **, $p < 0.01$.

Supplemental Figure 7. Cardiomyocyte Beclin 1 expression levels affect doxorubicin-induced cardiac fibrosis. (**A**) Representative trichrome stain images of hearts from WT and *Beclin 1*$^{+/-}$ mice treated with NS or DOX. *Beclin 1*$^{+/-}$ mice manifested reduced interstitial fibrosis relative to WT mice after chronic doxorubicin treatment. **(B)** Representative trichrome stain images of hearts from WT and Beclin 1 Tg mice treated with NS and DOX. Beclin 1 Tg mice showed increased perivascular and interstitial fibrosis relative to WT mice after chronic doxorubicin treatment. Scale bar, 100 μm.

Supplemental Table 1. Primers used in the study

Gene (Mouse)	Sequence
Anf	5-CTTCTTCCTCTTCCTGGCCT-3
	5-TTCATCGGTCTGCTCGCTCA-3
Bnp	5-TCCTTAATCTGTCGCCGCTG-3
	5-AGGCGCTGTCTTGAGACCTA-3
Col1a1	5-TGGCCAAGAAGACATCCCTGAAGT-3
	5-ACATCAGGTTTCCACGTCTCACCA-3
Ctgf	5-GTTGATGAGGCAGGAAGG-3
	5-AACTGAATGGAGTCCTAC-3
Beclin1	5-CAGGAGCTGGAAGATGTGGA-3
	5-GTGCCAGATATGGAAGGTCG-3
Sqstm1	5-CTTCAGCTTCTGCTTCA-3
	5-GGCACTCCTTCTTCTCTT-3
Bnip3	5-ATTGGTCAAGTCGGCCAGAA-3
	5-AGTCGCTGTACGCTTTGGGT-3
Gabarapl1	5-CATCGTGGAGAAGGCTCCTA-3
	5-ATACAGCTGTCCCATGGTAG-3
Lc3b	5-CGTCCTGGACAAGACCAAGT-3
	5-AGTGCTGTCCCGAACGTCTC-3
Atg5	5-GTGCTTCGAGATGTGTG-3
	5-AAGAGCTGAACTTGATGC-3
Atg12	5-AGATTCAGAGGTTGTGCTGC-3
	5-CAATGAGTCCTTGGATGGTC-3

Supplemental Table 2. Echocardiography of WT and *Beclin 1*$^{+/-}$

Genotype	Treatment	LVIDd(mm)	LVIDs(mm)	FS(%)	HR(bpm)
WT	NS	2.658±0.061	1.029±0.052	61.24±2.25	666±16
Beclin 1$^{+/-}$	NS	2.706±0.085	1.080±0.073	60.38±1.66	706±12
WT	DOX	2.909±0.037 *	1.413±0.065 *	51.49±2.93 *	675±14
Beclin 1$^{+/-}$	DOX	2.698±0.075	1.128±0.067 #	58.31±3.42 #	685±6

*, $p < 0.05$ WT-NS group VS WT-DOX group. #, $p < 0.05$ WT-DOX group VS *Beclin 1*$^{+/-}$ -DOX group

Supplemental Table 3. Echocardiography of WT and Beclin1 Tg

Genotype	Treatment	LVIDd(mm)	LVIDs(mm)	FS(%)	HR(bpm)
WT	NS	2.666±0.058	1.028±0.026	61.34±2.52	722±9
Beclin1 Tg	NS	2.730±0.060	1.037±0.03	62.08±3.44	717±11
WT	DOX	2.836±0.042	1.361±0.068 *	51.78±3.33 *	680±11
Beclin1 Tg	DOX	3.134±0.083 #	1.715±0.108 #	44.94±2.83 #	668±9

*, $p < 0.05$ WT-NS group VS WT-DOX group. #, $p < 0.05$ WT-DOX group VS Beclin1 Tg -DOX group